

# Computer Vision Self-supervised Learning Methods on Time Series

Daesoo Lee<sup>1\*</sup> and Erlend Aune<sup>1,2</sup>

<sup>1\*</sup>Department of Mathematical Sciences, Norwegian University of  
Science and Technology, Trondheim, Norway.

<sup>2</sup>Abelee, Oslo, Norway.

## Abstract

Self-supervised learning (SSL) has had great success in both computer vision. Most of the current mainstream computer vision SSL frameworks are based on Siamese network architecture. These approaches often rely on cleverly crafted loss functions and training setups to avoid feature collapse. In this study, we evaluate if those computer-vision SSL frameworks are also effective on a different modality (*i.e.*, time series). The effectiveness is experimented and evaluated on the UCR and UEA archives, and we show that the computer vision SSL frameworks can be effective even for time series. In addition, we propose a new method that improves on the recently proposed VICReg method. Our method improves on a *covariance* term proposed in VICReg, and in addition we augment the head of the architecture by an iterative normalization layer that accelerates the convergence of the model.

**Keywords:** Self-supervised learning, Time series, VICReg, VIBCReg

## 1 Introduction

In recent years, representation learning has had great success within computer vision, improving both on SOTA for fine-tuned models and achieving close-to SOTA results on linear evaluation on the learned representations [1–7], and many more. The main idea in these papers is to train a high-capacity neural network using a self-supervised learning (SSL) loss with a Siamese network’s architectural style [8]. The SSL loss is able to produce representations

of images that are useful for downstream tasks such as image classification and segmentation.

Most mainstream SSL frameworks have been developed in computer vision, and SSL for time series problems has seen much less attention despite their evident abundance in industrial, financial, and societal applications. The Makridakis competitions [9, 10] give examples of important econometric forecasting challenges. The UCR archive [11] is a collection of univariate time series datasets where classification is of importance, and in the industrial setting, sensor data and Internet of Things (IoT) data are examples where proper machine learning tools for time series modeling is important. The UEA archive [12] was designed as a first attempt to provide a standard archive for multivariate time series classification similar to UCR.

Our main focus is to test if the computer-vision SSL methods are also effective on time series so that we can potentially bring some of the quality ideas from the computer-vision representation learning literature to that of the time series. Thus, we investigate the mainstream SSL frameworks from computer vision and their effectiveness on time series datasets along with SSL frameworks for time series, and show that the computer-vision SSL frameworks are effective not only on images but also on time series. Also, we propose a new SSL framework named VIBCReg (Variance-Invariance-better-Covariance Regularization) which is based on VICReg and inspired by the feature decorrelation methods from [7, 13, 14]. VIBCReg can be viewed as an upgraded version of VICReg by having better covariance regularization.

The recent mainstream SSL frameworks can be divided into two main categories: 1) contrastive learning method, 2) non-contrastive learning method. The representative contrastive learning methods such as MoCo [3] and SimCLR [15] use positive and negative pairs and they learn representations by pulling the representations of the positive pairs together and pushing those of the negative pairs apart. However, these methods require a large number of negative pairs per positive pair to learn representations effectively. To eliminate the need for negative pairs, non-contrastive learning methods such as BYOL [4], SimSiam [5], Barlow Twins [6], and VICReg [7] have been proposed. Since non-contrastive learning methods use positive pairs only, their training setup could be simplified. Non-contrastive learning methods are also able to outperform the existing contrastive learning methods.

To further improve the quality of the learned representations, feature whitening and feature decorrelation have been main ideas behind some recent improvements [6, 7, 13, 14]. Initial SSL frameworks such as SimCLR suffer from a problem called feature collapse. When not enough negative pairs are available, the representations collapse to constant vectors. The collapse occurs since a similarity metric is still high even if all the features converged to constants, which is the reason for the use of the negative pairs to prevent feature collapse. Feature collapse has been partially resolved by using a momentum encoder [4], an asymmetric framework with a predictor, and stop-gradient [4, 5], which have popularized the non-contrastive learning methods. However,

one of the latest SSL frameworks, VICReg, shows that none of them is needed and that it is possible to conduct effective representation learning with the simplest Siamese architecture without the collapse via feature decorrelation. Using this idea for SSL has first shown up in W-MSE [13] recently, where the feature components are decorrelated from each other by whitening. Later, Barlow Twins encodes feature decorrelation by reducing off-diagonal terms of its cross-correlation matrix to zero. Hua et al. [14] encodes the feature decorrelation by introducing Decorrelated Batch Normalization (DBN) [16] and Shuffled-DBN. VICReg handles feature decorrelation by introducing variance and covariance regularization terms in its loss function in addition to a similarity loss.

The computer-vision SSL frameworks investigated in this paper are SimCLR, BYOL, SimSiam, Barlow Twins, and VICReg along with our proposal, VibCReg.

The SSL frameworks are evaluated 1) on a subset of UCR by linear and fine-tuning evaluation, and 2) on the UCR and UEA archives with the SVM (support vector machine) evaluation suggested in [17]. The SVM evaluation is conducted by fitting an SVM classifier on learned representations. As for the subset of UCR, ten datasets of the UCR archive with the highest number of time series within them and five datasets of the UCR archive with the highest number of labels are used.

## 2 Related Works

### 2.1 Contrastive Learning Methods

#### *Siamese Architecture-based SSL Frameworks*

We illustrate in Fig. 1 a comparison between several Siamese neural network [18] SSL frameworks. The Siamese neural network has two branches with a shared encoder on each side, and its similarity metric is computed based on two representations from the two encoders. Its main purpose is to learn representations such that two representations are similar if two input images belong to the same class and two representations are dissimilar if two input images belong to different classes. One of the main applications of the Siamese neural network is one-shot and few-shot learning for image verification [8, 18] where a representation of a given image can be obtained by an encoder of a trained Siamese neural network and is compared with representations of the existing images for the verification by a similarity metric. It should be noted that the Siamese neural network is trained in a supervised manner with a labeled dataset. The learning process of the representations by training an encoder is termed representation learning.

Although representation learning can be conducted using the Siamese neural network, its capability is somewhat limited by the fact that it utilizes supervised learning where a labeled dataset is required. To eliminate the need for a labeled dataset and still be able to conduct effective representation learning, SSL has become very popular where unlabeled datasets are utilized to train an encoder. Some of the representative contrastive learning methods that are

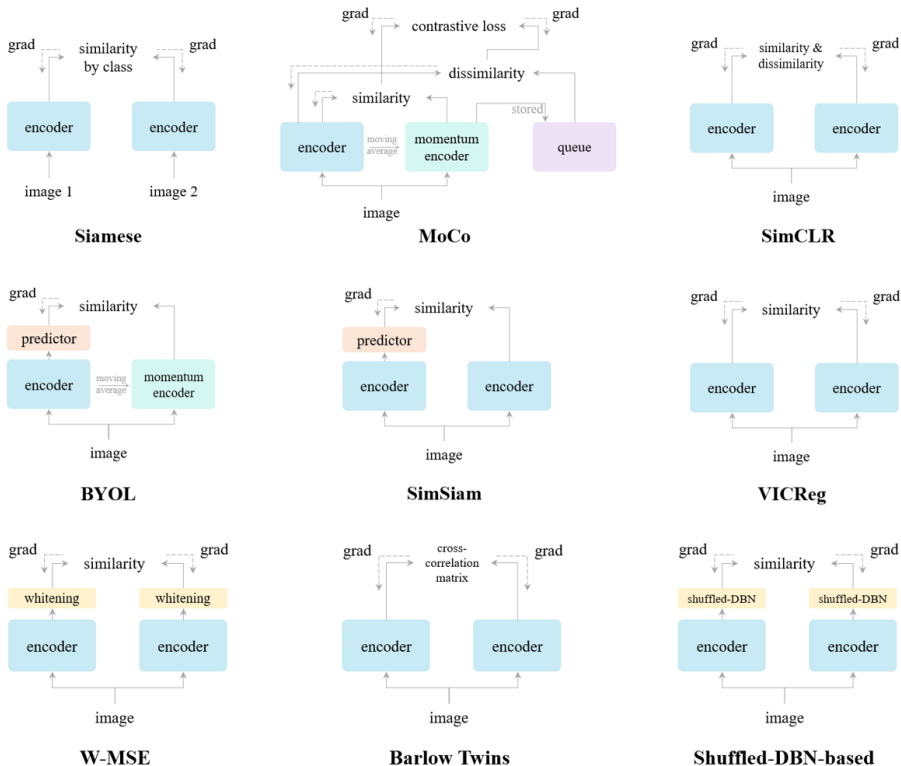


**Fig. 1** Comparison on Siamese architecture-based SSL frameworks. Siamese denotes the Siamese architecture [8] and the others are SSL frameworks. The encoder includes all layers that can be shared between both branches. The dash lines indicate the gradient propagation flow. Therefore, the lack of a dash line denotes stop-gradient.

based on the Siamese architecture are MoCo and SimCLR. Both frameworks are illustrated in Fig. 1.

**MoCo** is a contrastive learning method that requires a large number of negative pairs per positive pair, and MoCo keeps a large number of negative pairs by having a queue where a current mini-batch of representations is enqueued and the oldest mini-batch of representations in the queue is dequeued. A similarity loss is computed using representations from the encoder and the momentum encoder, and the dissimilarity loss is computed using representations from the encoder and the queue, and they are merged to form a form of a contrastive loss function, called InfoNCE [19]. The momentum encoder is a moving average of the encoder and it maintains consistency of the representations.

**SimCLR** greatly simplifies a framework for contrastive learning. Its major components are 1) a projector after a ResNet backbone encoder [20], 2) InfoNCE based on a large mini-batch. The projector is a small neural network that maps representations to the space where contrastive loss is applied. By having this, quality of representations is improved by leaving the downstream

task to the projector while the encoder is trained to output better quality representations.

### *SSL Frameworks for Time Series*

TNC is a recent SSL method to learn representations for non-stationary time series. It learns time series representations by ensuring that a distribution of signals from the same neighborhood is distinguishable from a distribution of non-neighboring signals. It was developed to address time series in the medical field, where modeling the dynamic nature of time series data is important.

## 2.2 Non-Contrastive Learning Methods

The representative non-contrastive learning methods are BYOL and SimSiam. Both frameworks are illustrated in Fig. 1.

**BYOL** has gained great popularity by proposing a framework that does not require any negative pair for the first time. Before BYOL, a large mini-batch size was required [15] or some kind of memory bank [3, 21] was needed to keep a large number of negative pairs. Grill et al. [4] hypothesized that BYOL may avoid the collapse without a negative pair due to a combination of 1) addition of a predictor to an encoder, forming an asymmetrical architecture and 2) use of the momentum encoder.

**SimSiam** can be viewed as a simplified version of BYOL where the momentum encoder is removed. Chen and He [5] empirically showed that a stop-gradient is critical to prevent the collapse.

### *Feature Decorrelation Considered*

The frameworks that improve the representation learning using the idea of feature decorrelation are W-MSE, Barlow Twins, and a Shuffled-DBN-based framework. They are illustrated in Fig. 1.

**W-MSE**'s core idea is to whiten feature components of representations so that the feature components are decorrelated from each other, which can eliminate feature redundancy. The whitening process used in W-MSE is based on a Cholesky decomposition [22] proposed by Siarohin et al. [23].

**Barlow Twins** encodes a similarity loss (invariance term) and a loss for feature decorrelation (redundancy reduction term) into the cross-correlation matrix. The cross-correlation is computed by conducting matrix multiplication of  $z_i^T z_j$  where  $z_i \in \mathbb{R}^{B \times F}$  and  $z_j \in \mathbb{R}^{B \times F}$  and  $B$  and  $F$  denote batch size and feature size, respectively. Then, representation learning is conducted by optimizing the cross-correlation matrix to be an identity matrix, where optimization of the diagonal terms corresponds to that of a similarity loss and optimization of the off-diagonal terms corresponds to that of the feature decorrelation loss.

**DBN-based framework**'s authors [14] categorized the feature collapse into two categories: 1) *complete collapse*, caused by constant feature components, 2) *dimensional collapse*, caused by redundant feature components. They pointed out that previous works had mentioned and addressed the complete

collapse only but not the dimensional collapse. Its main idea is to use DBN to normalize the output from its encoder-projector, which provides the feature decorrelation effect, and the feature decorrelation prevents the dimensional collapse. To further decorrelate the features, Shuffled-DBN is proposed, in which an order of feature components is randomly arranged before DBN and the output is rearranged back to the original feature-wise order.

### ***Feature Decorrelation and Feature-component Expressiveness Considered***

**VICReg** encodes *Feature Decorrelation* (FD) and *Feature-component Expressiveness* (FcE) in its loss function in addition to a similarity loss, where FD and FcE are termed *variance term* and *covariance term* in VICReg, respectively. A high FcE indicates that output values from a feature component have a high variance and vice versa. Hence, a (near)-zero FcE indicates the complete collapse. Its strength lies in its simplicity, VICReg uses the simplest Siamese form and does not require either the stop-gradient, asymmetrical architecture, or whitening/normalization layer. Despite its simplicity, its performance is very competitive compared to other latest SSL frameworks.

## **2.3 Time Series Classification Methods**

In the time series classification (TSC) literature, [17, 24] propose scalable and transferable unsupervised representation learning frameworks and [25] proposes an unsupervised representation learning framework that is only scalable but not transferable. [24] proposes TimeNet which is an autoencoder based on the seq2seq model [26]. [17] proposes a contrastive unsupervised learning method that uses a triplet loss. One of the main findings in TimeNet is that an encoder pretrained on many different datasets learns to effectively capture important characteristics of time series so that the pretrained encoder can also capture the important characteristics of time series of an unseen dataset. [17] further improved a quality of learned representations by introducing a modified TCN (temporal convolutional network) [27] to cover a large receptive field and a contrastive learning approach. [17] also shows that its pretrained encoder has good transferability of its learned representations. Although ROCKET [25] produces representations that result in good classification performance, its representation size requires to be 20,000 which is extremely large compared to any of the typical representation learning methods (*i.e.*, typically maximum 512) [2–7]. The large representation size limits a choice of a classifier. Also ROCKET’s representations are not transferable from one dataset to another dataset unlike [17, 24]. Hence, TimeNet and the Franceschi are chosen to the main competing framework in our study.

## **3 Proposed Method**

VibCReg (Variance-Invariance-better-Covariance Regularization) is inspired by VICReg (Variance-Invariance-Covariance Regularization), and can be

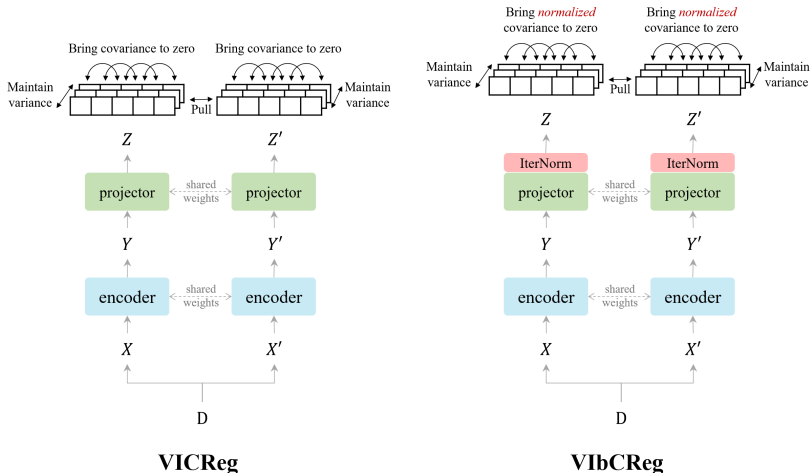


**Fig. 2** Comparison between VICReg and VibCReg, where the difference is highlighted in red. As for VibCReg, two batches of different views  $X$  and  $X'$  are taken from a batch of input data  $D$ , and representations  $Y$  and  $Y'$  are obtained through the encoder. Then, the representations are projected to a higher dimension via the projector and the iterative normalization (IterNorm) layer, yielding  $Z$  and  $Z'$ . Then, similarity between  $Z$  and  $Z'$  and variance along the batch dimension are maximized, while feature components of  $Z$  and  $Z'$  are decorrelated from each other.

viewed as VICReg with a better covariance regularization. It should be noted that the variance, invariance, and covariance terms in VICReg correspond to what we call the *feature component expressiveness* (FcE), similarity loss, and *feature decorrelation* (FD) terms in VibCReg, respectively. By having better covariance regularization, VibCReg outperforms VICReg in terms of learning speed, linear evaluation, and semi-supervised training. What motivated VibCReg are the followings: 1) FD has been one of the key components for improvement of quality of learned representations [6, 7, 13, 16], 2) Hua et al. [14] showed that application of DBN and Shuffled-DBN on the output from an encoder-projector is very effective for faster and further FD, 3) addressing FcE in addition to FD is shown to be effective [7], 4) scale of the VICReg’s FD loss (covariance term) varies depending on feature size and its scale range is quite wide due to its summation over the covariance matrix. Hence, we assumed that the scale of the VICReg’s FD loss could be modified to be consistent and have a small range so that a weight parameter for the FD loss would not have to be re-tuned in accordance with a change of the feature size.

VibCReg is illustrated in Fig. 2 in comparison to VICReg. In Fig. 2, the two views,  $X$  and  $X'$ , are encoded using the encoder into representations  $Y$  and  $Y'$ . The representations are further processed by the projector and an iterative normalization (IterNorm) layer [28] into projections  $Z$  and  $Z'$ . The loss is computed at the projection level on  $Z$  and  $Z'$ .

We describe here a loss function of VibCReg, which consists of a similarity loss, FcE loss, and FD loss. It should be noted that the similarity loss and the FcE loss are defined the same as in VICReg. The input data is processed

in batches, and we denote  $Z = [z_1, \dots, z_B]^T \in \mathbb{R}^{B \times F}$  and  $Z' = [z'_1, \dots, z'_B]^T \in \mathbb{R}^{B \times F}$  where  $B$  and  $F$  denote batch size and feature size, respectively. The *similarity loss (invariance term)* is defined as Eq. (1). The *FcE loss (variance term)* is defined as Eq. (2), where  $\text{Var}(\cdot)$  denotes a variance estimator,  $\gamma$  is a target value for the standard deviation, fixed to 1 in our experiments,  $\epsilon$  is a small scalar (*i.e.*, 0.0001) preventing numerical instabilities.

$$s(Z, Z') = \frac{1}{B} \sum_{b=1}^B \|Z_b - Z'_b\|_2^2 \quad (1)$$

$$v(Z) = \frac{1}{F} \sum_{f=1}^F \text{ReLU} \left( \gamma - \sqrt{\text{Var}(Z_f) + \epsilon} \right) \quad (2)$$

The *FD loss* is the only component of VIbCReg’s loss that differs from the corresponding *covariance term* in the loss of VICReg, thus, we present here a comparison between the two. The covariance matrix of  $Z$  in VICReg is defined as Eq. (3), and the covariance matrix in VIbCReg is defined as Eq. (4) where the  $\ell_2$ -norm is conducted along the batch dimension. Then, the FD loss of VICReg is defined as Eq. (5) and that of VIbCReg is defined as Eq. (6). Eq. (4) constrains the terms to range from -1 to 1, and Eq. (6) takes a mean of the covariance matrix by dividing the summation by a number of the matrix elements. Hence, Eq. (4) and Eq. (6) keep a scale and a range of the FD loss neat and small.

$$C(Z)_{\text{VICReg}} = \frac{1}{B-1} (Z - \bar{Z})^T (Z - \bar{Z}) \quad \text{where } \bar{Z} = \frac{1}{B} \sum_{b=1}^B Z_b \quad (3)$$

$$C(Z)_{\text{VIbCReg}} = \left( \frac{Z - \bar{Z}}{\|Z - \bar{Z}\|_2} \right)^T \left( \frac{Z - \bar{Z}}{\|Z - \bar{Z}\|_2} \right) \quad (4)$$

$$c(Z)_{\text{VICReg}} = \frac{1}{F} \sum_{i \neq j} C_{\text{VICReg}}(Z)_{i,j}^2 \quad (5)$$

$$c(Z)_{\text{VIbCReg}} = \frac{1}{F^2} \sum_{i \neq j} C_{\text{VIbCReg}}(Z)_{i,j}^2 \quad (6)$$

The overall loss function is a weighted average of the similarity loss, FcE loss, and FD loss:

$$l(Z, Z') = \lambda s(Z, Z') + \mu \{v(Z) + v(Z')\} + \nu \{c(Z) + c(Z')\} \quad (7)$$

where  $\lambda$ ,  $\mu$ , and  $\nu$  are hyper-parameters controlling the importance of each term in the loss.

Another key component in VIbCReg is *IterNorm*. [14] showed that applying DBN on the output from an encoder-projector could improve representation



learning, emphasizing that the whitening process helps the learning process, which corresponds to a main argument in the DBN paper [16]. To further improve DBN, IterNorm was proposed [28]. IterNorm was verified to be more efficient for whitening than DBN by employing Newton’s iteration to approximate a whitening matrix. Therefore, we employ IterNorm instead of DBN, and IterNorm is applied to the output from an encoder-projector as shown in Fig. 2. Then, feature decorrelation is strongly supported, induced by the following two factors: 1) IterNorm, 2) optimization of the FD loss.

### Relation to VICReg

To summarize, VIBcReg can be viewed as VICReg with the normalized covariance matrix (instead of the covariance matrix) and IterNorm.

Theoretically, VIBcReg should produce representations that are better decorrelated. To show that, we present T-SNE visualization of learned representations with VICReg and VIBcReg for several datasets from the UCR archive in Fig. 3. For (a)-(f) and (h), it is apparent that VIBcReg’s representations are better in terms of class-separability. For (g) and (i), VIBcReg’s representations are more scattered out due to the stronger decorrelation. It may seem that VICReg’s representations are better separated but when looked closely, VICReg’s representations are quite mixed between two classes around the boundary line between the two classes unlike VIBcReg’s. This T-SNE result is well aligned with the linear evaluation result presented in Table 2.

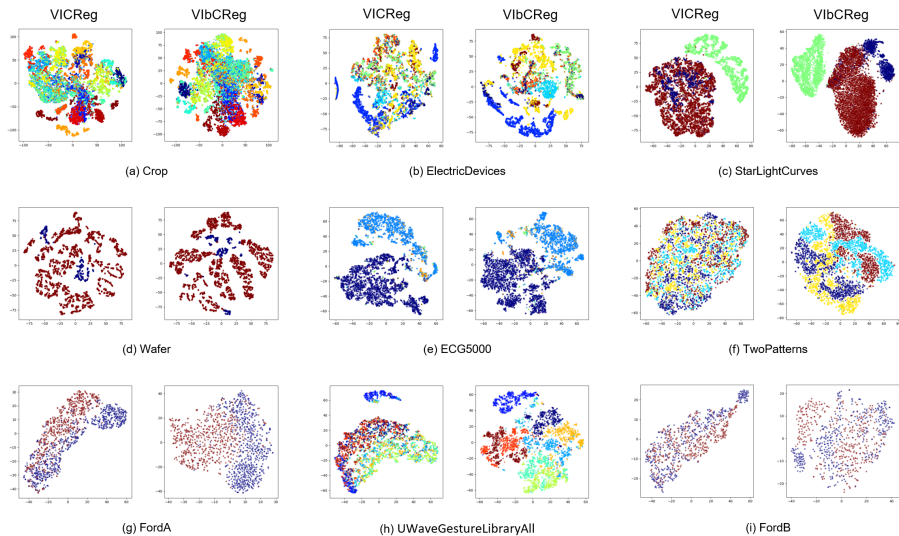


**Fig. 3** T-SNE visualization of learned representations with VICReg and VIBcReg, respectively. For each set of subfigures, the left subfigure is by VICReg and the right subfigure is by VIBcReg. A subset dataset name is shown below each set of the subfigures and the different colors represent different classes.

## 4 Experimental Evaluation

Our experimental evaluation consists of two parts: 1) evaluation according to the common protocol for SSL frameworks in computer vision, 2) The SVM evaluation [17]. In the part-1 evaluation, SimCLR, BYOL, SimSiam, Barlow Twins, VICReg, TNC, and ViBcReg are evaluated on a subset of the UCR archive. In the part-2 evaluation, all the computer-vision SSL frameworks (*e.g.*, SimCLR, BYOL, SimSiam, Barlow Twins, VICReg), ViBcReg are evaluated on the UCR and UEA archives compared to the Franceschi.

### *Encoder*

We follow the convention of the previous SSL papers by using ResNet [4–7] for an encoder. But since the dataset size is much smaller than the size for SSL in computer vision, we use a *light-weighted* 1D ResNet, inspired by [29]. The detailed architecture is illustrated in Appendix A1. It is used as an encoder for SimCLR, BYOL, SimSiam, Barlow Twins, VICReg, TNC, and ViBcReg.

### *Training*

We use the AdamW [30] ( $lr=0.001$ , weight decay=0.00001, batch size=256) optimizer, and 100 epochs of pretraining for the part-1 evaluation and 200 epochs for the part-2 evaluation. We use a cosine learning rate scheduler [31]. Details of the data augmentation methods are described in Appendix A.3. We use PyTorch [32] and train our models on a single GPU (GTX1080-Ti).

## 4.1 Experimental Evaluation: Part 1

### *Datasets*

In this evaluation, the UCR archive is used, from which we select the 10 largest datasets together with the 5 datasets with more than 900 samples having the largest number of classes. For the UCR datasets, each dataset is split into 80% (training set) and 20% (test set) by a stratified split. A model pre-training by SSL is conducted and evaluated on each dataset. Therefore, the UCR datasets are independent of one another in our experiments. As for the preprocessing, the UCR datasets are preprocessed by z-normalization followed by arcsinh. Summary of the UCR datasets is presented in Table 1.

### *Linear Evaluation*

We follow the linear evaluation protocols from the computer vision field [4–7, 33]. Given the pre-trained encoder, we train a supervised linear classifier on the frozen features from the encoder. The features are from the ResNet’s global average pooling (GAP) layer. Experimental results for the linear evaluation on the UCR datasets are presented in Table 2. For the linear classifier’s training, the same optimizer and the same learning rate scheduler are used with training epochs of 50. Details of the data augmentation methods are described in Appendix A.3.

**Table 1** Summary of the UCR datasets. The first 10 datasets are the 10 largest datasets from the UCR archive, and the second 5 datasets are the datasets with the 5 largest number of classes from the UCR archive, where a dataset has more than 900 samples.

Dataset name	#Samples	#Classes	Length
Crop	24000	24	46
ElectricDevices	16637	7	96
StarLightCurves	9236	3	1024
Wafer	7164	2	152
ECG5000	5000	5	140
TwoPatterns	5000	4	128
FordA	4921	2	500
UWaveGestureLibraryAll	4478	8	945
FordB	4446	2	500
ChlorineConcentration	4307	3	166
ShapesAll	1200	60	512
FiftyWords	905	50	270
NonInvasiveFetalECGThorax1	3765	42	750
Phoneme	2110	39	1024
WordSynonyms	905	25	270

The linear evaluation result on the UCR subset datasets shows that VlbCReg performs the best among the competing SSL frameworks and it even performs very close or outperforms the supervised one on many of the datasets, which indicates that quality of the learned representations by VlbCReg is very good as shown in Fig. 3. The second best is SimCLR, which is interesting given that SimCLR was proposed before BYOL, SimSiam, Barlow Twins, and VICReg. The main difference of SimCLR from other methods such as BYOL, SimSiam, Barlow Twins, and VICReg is that it is a contrastive method, while the others are contrastive methods. A contrastive method usually induces stronger decorrelation by explicitly pushing apart between one sample and the rest of the samples in a batch in the representation space. The effect can be observed in Fig. C2, where SimCLR generally achieves low FD metric. The FD metric is for measuring the feature decorrelation. The low FD metric indicates high feature decorrelation. In the same sense, VlbCReg also provides strong feature decorrelation. Thus, we suppose that strong feature decorrelation is important for linear class-separability of learned representations.

### *Fine-tuning Evaluation on a Small Dataset*

Fine-tuning evaluation on a subset of training dataset is conducted to do the ablation study. We follow the ablation study protocols from the computer vision domain [4–7, 33]. Given the pre-trained encoder, we fine-tune the pre-trained encoder and train the linear classifier. Experimental results for the fine-tuning evaluation on the UCR datasets are presented in Table 3. AdamW optimizer is used with ( $lr_{enc}=0.0001$ ,  $lr_{cls}=0.001$ , batch size=256,

**Table 2** Linear evaluation on the UCR datasets. The results are obtained over 5 runs with different random seeds for the stratified split. It is noticeable that the proposed frameworks outperform the other frameworks with significant margins, and they even outperform **Supervised** on some datasets. The values within the parentheses are standard deviations. Note that **Rand Init** denotes a randomly-initialized frozen encoder with a linear classifier on the top and **Supervised** denotes a trainable encoder-linear classifier trained in a supervised manner.

Dataset Name	Rand Init	SimCLR	BYOL	SimSiam	Barlow Twins	VICReg	TNC	VibCReg	Supervised
Crop	49.6(0.1)	65.6(1.2)	67.8(0.8)	56.0(0.8)	63.7(0.7)	66.2(9.5)	61.6(2.1)	<b>71.0(0.7)</b>	80.1(0.4)
ElectricDevices	51.2(0.7)	<b>87.7(0.4)</b>	83.1(1.1)	53.2(4.3)	64.1(1.1)	73.6(0.1)	69.3(1.1)	87.1(0.3)	87.0(0.2)
StarLightCurves	76.7(2.3)	97.4(0.4)	97.7(0.1)	71.3(8.5)	88.7(4.2)	97.5(0.1)	97.0(0.7)	<b>97.8(0.1)</b>	98.3(0.1)
Wafer	89.4(0.0)	93.2(1.2)	99.4(0.5)	98.4(0.4)	95.9(0.4)	98.8(0.2)	<b>99.5(0.0)</b>	<b>99.5(0.1)</b>	99.9(0.0)
ECG5000	72.9(11.5)	94.8(0.1)	94.1(0.2)	83.1(5.5)	90.9(1.2)	92.8(0.0)	93.3(0.3)	<b>95.4(0.1)</b>	95.8(0.1)
TwoPatterns	42.8(1.6)	<b>99.4(0.2)</b>	69.4(18.1)	37.9(4.4)	87.2(6.5)	81.2(0.6)	92.1(1.4)	<b>99.3(0.2)</b>	100.0(0.0)
FordA	54.5(0.9)	95.1(0.0)	93.6(0.2)	83.0(4.1)	74.5(4.3)	79.0(0.3)	72.0(3.5)	<b>95.5(0.3)</b>	93.3(0.3)
UMWaveGestureLibraryAll	47.2(1.3)	86.3(1.2)	89.7(1.0)	30.3(6.8)	51.3(5.6)	57.5(0.8)	64.8(1.6)	<b>90.9(0.4)</b>	96.2(0.4)
FordB	65.7(1.1)	90.5(4.9)	94.0(0.2)	60.8(5.4)	76.1(1.6)	85.4(0.3)	64.5(3.5)	<b>94.0(0.3)</b>	92.4(0.5)
ChlorineConcentration	53.6(0.0)	62.1(1.9)	57.4(0.4)	53.7(0.0)	55.5(0.3)	55.5(0.1)	55.3(0.8)	<b>65.2(0.7)</b>	100.0(0.0)
ShapesAll	7.9(2.5)	80.7(3.4)	70.8(1.5)	14.1(3.1)	39.2(3.6)	31.2(2.4)	51.8(4.5)	<b>85.7(0.8)</b>	91.2(1.0)
FiftyWords	13.6(1.7)	46.8(2.2)	30.0(0.3)	15.8(2.1)	25.4(1.7)	26.3(0.9)	26.2(2.6)	<b>50.2(1.1)</b>	77.2(1.2)
NonInvasiveFetalECGThorax1	5.0(0.8)	51.9(3.5)	<b>60.8(10.6)</b>	20.0(3.6)	21.4(8.8)	37.6(0.7)	58.0(4.5)	<b>58.5(0.6)</b>	94.5(0.3)
Phoneme	11.1(0.0)	41.3(0.1)	38.9(1.1)	18.1(0.6)	19.9(1.5)	21.4(0.2)	28.0(2.2)	<b>42.8(0.5)</b>	47.8(1.0)
WordSynonyms	22.1(0.9)	<b>43.8(0.5)</b>	29.1(0.3)	24.4(0.4)	29.0(1.3)	23.8(0.3)	28.9(2.5)	<b>46.7(0.7)</b>	73.7(1.8)
Mean Rank	7.7	2.7	2.8	6.7	5.5	4.7	4.7	1.3	

weight decay=0.001, training epochs=100), where  $lr_{enc}$  and  $lr_{cls}$  denote learning rates for the encoder and the linear classifier, respectively. During the fine-tuning, the BN statistics are set such that they can be updated. Details of the data augmentation methods are described in Appendix A.3.

Similar to the linear evaluation result on the UCR, VIbCReg performs the best among the competing SSL frameworks in the fine-tuning evaluation on the UCR and beats the supervised one in the small-dataset regimes. Although SimCLR is the second best in the linear evaluation, it is not in the fine-tuning evaluation. VICReg performs the second best here. This indicates that VICReg’s learned representations are easily adaptable to incoming data. The order mismatch in between linear evaluation and fine-tuning evaluation can also be found in [34], therefore, it is not uncommon to observe.

### ***Faster Representation Learning by VIbCReg***

On top of the better performance, VIbCReg has another strength: *faster representation learning*, which makes VIbCReg more appealing compared to its competitors. The speed of representation learning is presented by kNN classification accuracy for the UCR datasets [5] in Fig. 4 along with *FD metric*  $\mathcal{M}_{FD}$  and *FcE metric*  $\mathcal{M}_{FcE}$ . The FD metric and FcE metric are metrics for the feature decorrelation and feature component expressiveness. The low FD metric indicates high feature decorrelation (*i.e.*, features are well decorrelated) and vice versa. The low FcE metric indicates the feature collapse and vice versa. Note that VIbCReg is trained to have the FcE metric of 1. Details of both metrics are specified in Appendix B. To keep this section neat, the corresponding FD and FcE metrics of Fig. 4 is presented in Appendix C. It is recognizable that VIbCReg shows the fastest convergence and the highest kNN accuracy on most of the datasets.

**Table 3** Fine-tuning evaluation on subsets of the UCR datasets. The results are obtained over 5 runs with different random seed for the stratified split. In 5% and 10%, results on some datasets missing because the split training subsets are too small.

Dataset name	SimCLR	BYOL	SimSiam	Barlow Twins	VICReg	TNC	VibCReg	Supervised
<i>Fine-tuning evaluation on 5% of the training dataset</i>								
Crop	47.7(1.1)	59.3(0.3)	61.6(0.6)	60.5(0.5)	61.6(2.4)	50.0(2.1)	62.4(0.3)	62.6(0.7)
ElectricDevices	82.1(0.7)	74.5(1.2)	71.4(2.8)	69.2(1.5)	73.1(0.3)	52.8(2.7)	84.7(0.4)	69.0(0.9)
StarLightCurves	91.6(1.1)	95.0(1.7)	85.3(0.1)	93.0(4.3)	98.1(0.1)	85.9(0.5)	98.1(0.2)	97.8(0.2)
Wafer	89.3(0.1)	90.3(1.5)	89.3(0.1)	98.8(0.1)	99.4(0.1)	99.7(0.8)	99.1(0.2)	99.3(0.2)
ECG5000	92.8(0.2)	91.9(1.0)	91.4(1.2)	91.8(0.8)	94.0(0.5)	91.4(1.3)	94.1(0.6)	94.1(0.4)
TwoPatterns	91.6(0.5)	37.1(8.4)	49.3(8.5)	96.2(2.2)	98.6(0.4)	99.2(3.7)	88.0(4.2)	88.0(4.2)
FordA	<b>94.4(0.9)</b>	93.6(1.0)	91.1(1.0)	80.6(3.5)	90.1(0.6)	66.8(5.3)	94.4(0.6)	89.8(1.0)
UWaveGestureLibraryAll	70.9(1.8)	75.3(2.0)	42.9(11.3)	55.1(4.6)	77.1(2.2)	53.3(1.6)	83.4(2.3)	78.5(1.1)
FordB	91.8(0.7)	91.2(0.4)	74.3(5.3)	82.4(2.1)	90.0(0.4)	60.5(5.3)	92.2(0.7)	87.4(1.9)
ChlorineConcentration	52.7(1.0)	52.0(2.4)	57.4(0.7)	55.9(0.5)	56.7(1.0)	61.7(0.6)	61.7(1.7)	65.6(1.9)
NonInvasiveFetalECGThorax1	--	40.5(13.0)	--	21.2(6.1)	44.2(2.6)	--	45.6(1.9)	<b>66.9(3.8)</b>
<i>Fine-tuning evaluation on 10% of the training dataset</i>								
Crop	54.4(0.8)	62.3(1.1)	66.2(0.6)	65.3(0.4)	66.4(1.1)	54.4(2.9)	66.3(0.4)	67.0(0.7)
ElectricDevices	83.3(0.3)	77.2(1.6)	75.1(1.9)	73.8(0.8)	75.9(0.5)	60.9(2.5)	86.5(0.6)	73.4(0.7)
StarLightCurves	94.8(0.1)	96.6(0.6)	91.8(5.3)	97.4(0.3)	98.2(0.1)	88.3(1.7)	98.2(0.1)	98.0(0.2)
Wafer	89.3(0.2)	93.1(3.3)	<b>99.6(0.1)</b>	99.4(0.1)	<b>99.6(0.1)</b>	99.6(0.3)	99.5(0.1)	<b>99.6(0.1)</b>
ECG5000	93.3(0.1)	92.4(0.1)	93.2(0.3)	93.1(0.5)	94.6(0.7)	91.7(0.9)	95.0(0.5)	94.4(0.7)
TwoPatterns	94.9(0.7)	41.4(10.2)	93.0(5.0)	99.5(0.5)	99.7(0.1)	76.9(4.0)	99.9(0.1)	99.9(0.1)
FordA	94.5(0.4)	93.1(0.7)	92.4(0.1)	87.5(1.4)	92.8(0.3)	68.8(3.5)	94.8(0.2)	91.7(0.3)
UWaveGestureLibraryAll	75.5(1.4)	79.4(1.9)	58.1(14.0)	68.5(3.2)	84.9(1.0)	55.7(3.7)	91.2(1.2)	84.7(0.9)
FordB	92.1(0.9)	91.1(1.1)	89.3(0.6)	89.3(1.9)	91.3(0.6)	93.0(0.5)	89.1(0.3)	89.1(0.3)
ChlorineConcentration	54.4(1.6)	55.7(0.9)	63.4(0.7)	56.2(0.3)	60.6(1.3)	72.2(2.6)	76.7(2.2)	76.7(2.2)
ShapesAll	--	42.2(2.5)	--	35.4(3.4)	38.2(2.5)	25.8(1.9)	--	56.2(4.0)
NonInvasiveFetalECGThorax1	20.5(4.0)	31.3(12.6)	38.1(5.6)	24.4(3.7)	45.7(1.9)	12.2(0.9)	61.8(1.6)	77.4(4.1)
WordSynonyms	37.9(4.5)	28.5(4.2)	29.3(1.1)	34.4(2.5)	40.3(1.4)	27.6(6.0)	45.4(2.6)	36.2(2.4)
<i>Fine-tuning evaluation on 20% of the training dataset</i>								
Crop	58.2(0.7)	64.6(0.7)	70.4(0.5)	70.2(0.4)	70.4(1.3)	27.5(2.5)	70.6(0.5)	71.1(0.6)
ElectricDevices	58.7(0.0)	78.7(1.3)	80.0(0.9)	79.7(0.5)	79.0(0.2)	63.1(2.8)	88.1(0.3)	78.5(0.6)
StarLightCurves	96.7(0.2)	97.6(0.3)	98.0(0.3)	98.0(0.3)	<b>98.4(0.1)</b>	93.1(2.5)	98.3(0.1)	98.2(0.1)
Wafer	89.4(0.3)	97.8(0.6)	<b>99.7(0.1)</b>	<b>99.6(0.1)</b>	<b>99.6(0.1)</b>	99.6(0.3)	99.6(0.1)	<b>99.7(0.1)</b>
ECG5000	93.6(0.7)	93.0(0.2)	94.3(0.7)	94.4(0.2)	95.3(0.2)	92.4(0.2)	95.6(0.3)	95.3(0.2)
TwoPatterns	96.8(0.9)	42.2(10.3)	<b>99.9(0.1)</b>	<b>99.9(0.2)</b>	<b>100.0(0.0)</b>	84.2(2.5)	<b>100.0(0.0)</b>	<b>100.0(0.0)</b>
FordA	94.5(0.4)	93.3(0.4)	93.2(0.5)	91.2(0.5)	93.2(0.4)	70.4(3.9)	95.0(0.4)	92.2(0.6)
UWaveGestureLibraryAll	79.0(0.7)	83.0(1.4)	78.0(8.6)	85.5(1.4)	89.2(0.4)	59.1(2.7)	94.5(0.7)	89.7(1.0)
FordB	93.1(0.5)	91.6(1.0)	91.0(0.5)	91.8(0.4)	92.1(0.5)	90.8(0.3)	93.7(0.5)	90.8(0.3)
ChlorineConcentration	54.3(1.4)	56.4(1.4)	85.4(1.1)	56.7(0.7)	81.4(0.9)	56.6(7.4)	88.4(0.9)	88.4(0.9)
ShapesAll	73.6(2.9)	55.1(2.1)	27.6(11.2)	48.8(3.5)	53.6(0.6)	31.8(9.9)	<b>79.6(1.9)</b>	66.6(3.6)
FiftyWords	44.0(0.8)	29.1(1.2)	31.7(1.3)	47.1(1.9)	46.7(2.7)	25.0(1.1)	56.4(1.7)	49.0(1.9)
NonInvasiveFetalECGThorax1	35.2(2.9)	50.3(13.2)	72.9(3.2)	49.8(1.1)	79.7(1.1)	23.7(5.3)	83.0(0.8)	<b>87.4(0.7)</b>
Phoneme	35.1(0.5)	34.7(2.2)	27.5(2.0)	27.8(1.0)	34.5(1.1)	32.7(4.0)	<b>41.5(1.4)</b>	32.8(1.6)
WordSynonyms	39.8(1.0)	30.6(1.9)	32.7(4.9)	42.4(2.7)	47.7(3.3)	30.0(7.9)	55.9(2.9)	47.8(3.2)
Mean Rank	5.1	5.4	5.1	5.2	3.1	7.4	1.6	3.1

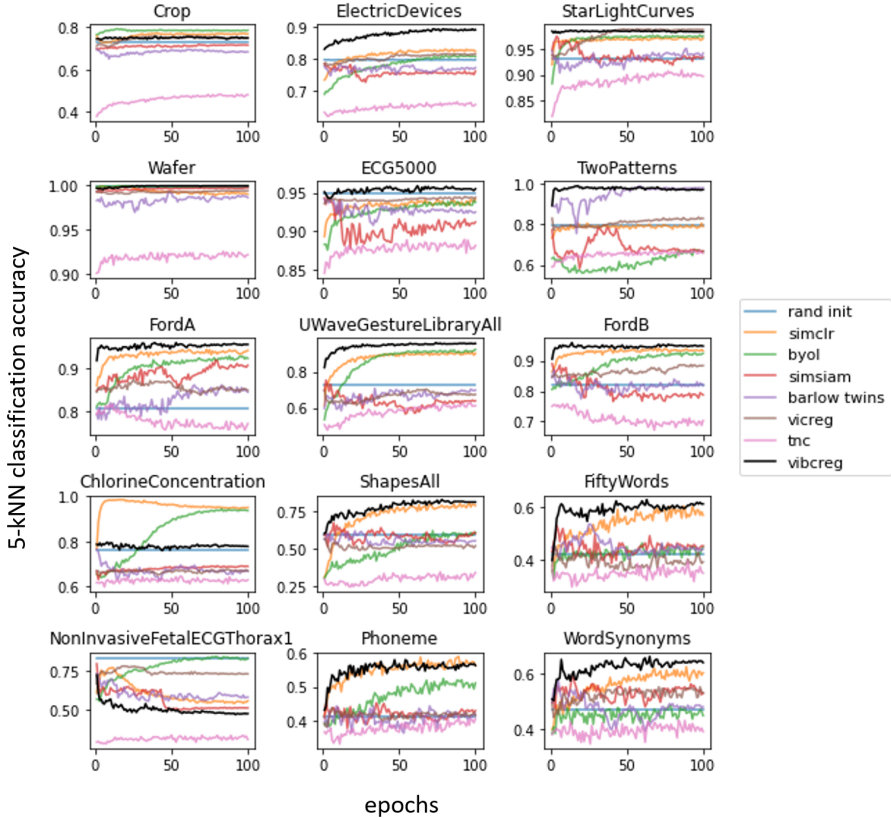


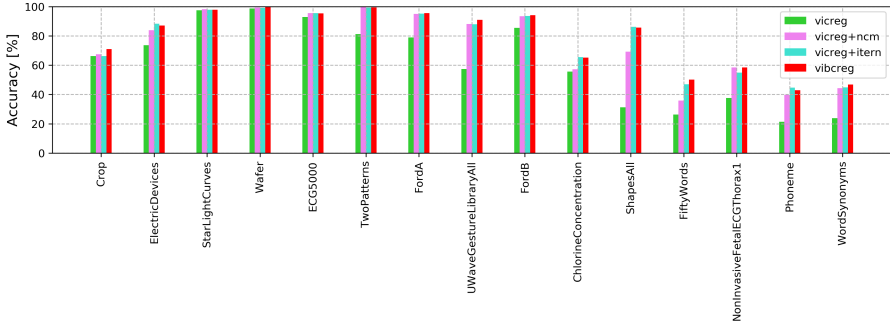
Fig. 4 5-kNN classification accuracy on the UCR datasets during the representation learning.

## 4.2 Between VICReg and VibCReg

As mentioned earlier in Section 3, VibCReg can be viewed as VICReg with the normalized covariance matrix (NCM) and IterNorm. In this subsection, frameworks between VICReg and VibCReg are investigated as shown in Table 4. The linear evaluation results of the four frameworks on the UCR datasets are presented in Fig. 5. It shows that either adding NCM (`ncm`) or IterNorm (`itern`) improves the performance. VibCReg shows the most consistently-high performance among the four frameworks.

**Table 4** Frameworks between VICReg and VibCReg: VICReg+NCM and VICReg+IterN.

Frameworks	Normalized Covariance Matrix	IterNorm	Notation
VICReg			VICReg
-	o		<i>VICReg+NCM</i>
-		o	<i>VICReg+IterN</i>
-	o	o	VibCReg

**Fig. 5** Comparative linear evaluation of the frameworks between VICReg and VibCReg.

### 4.3 Sensitivity Test w.r.t Weight for the FD Loss

The normalized covariance matrix is proposed to alleviate an effort for tuning the weight hyperparameter  $\nu$  for the feature decorrelation loss term  $c(Z)$ . Without the normalization, a scale of  $c(Z)$  from the covariance matrix can be significantly large and wide, which would make the tuning process harder. To show that the tuning process is easier with the normalized covariance matrix (*i.e.*, performance is relatively quite consistent with respect to  $\nu$ ), sensitivity test results with respect to  $\nu$  are presented in Fig. 6. It is apparent that the performance gaps between different  $\nu$  are much smaller for VibCReg than VICReg in general, which makes the tuning process for  $\nu$  much easier.



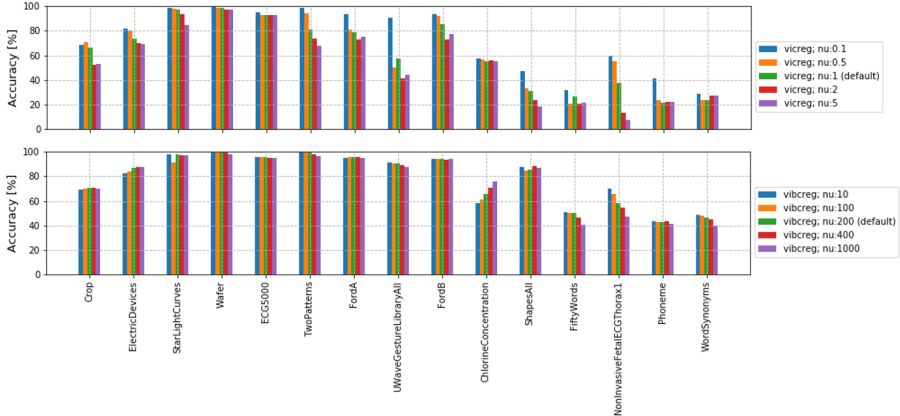


**Fig. 6** Linear evaluation of the sensitivity test with respect to  $\nu$ . Default values of  $\nu$  for VICReg and VIBcReg are 1 and 200, respectively. Variants of  $\nu$  are set by 5/10%, 50%, 200%, and 500% of the default values.

## 4.4 Experimental Evaluation: Part 2

### Datasets

The part-2 evaluation is conducted on the entire UCR and UEA archives except for a few datasets with varying length, significantly-short length such that an encoder cannot process, or missing values. The training and test datasets are used as given by the archives and dataset preprocessing follows the Franceschi which uses a simple z-normalization.

### SVM evaluation

An extensive experiment on the UCR and UEA archives was conducted by [17] and the SVM evaluation is used in their work. We follow the same evaluation process as [17] which is fitting a SVM-classifier on the learned representations with the penalty  $C \in \{10^i \mid i \in [-4, 4]\} \cup \{\infty\}$  and reporting the highest accuracy.

[17] reported several accuracies with respect to a different number of negative samples for each dataset. In our SVM evaluation result table, a mean of the accuracies is reported for the Franceschi. [17] also reported SVM accuracy based on a concatenated representation of all the representations from different encoders with a different number of negative samples but that accuracy is not used in our comparison because that accuracy is based on multiple different encoders (*i.e.*, 4 for UCR and 3 for UEA) that are trained separately.

Complete result tables on UCR and UEA are presented in Tables 5-6 and Table 7, respectively. There are several blank results on some UCR and UEA datasets for the computer-vision SSL framework and VIBcReg. That is due to the GPU memory issue caused by using two input pairs with crop length of 50% and 100% as described in Appendix A.3.

It can be observed that VIbCReg performs better than all the other computer-vision SSL frameworks and performs better than the Franceschi on the UCR and similar to the Franceschi on the UEA. Yet, given that VIbCReg uses a simpler encoder, simpler SSL framework, and compatible with image data, VIbCReg is more appealing than the Franceschi overall. For the encoder, VIbCReg uses the common encoder, ResNet, while the Franceschi uses a specifically-modified TCN encoder. For the SSL framework, a non-contrastive approach is simpler than a contrastive one because it does not require negative example sampling. In the Franceschi, the performance can vary significantly by a choice of number of negative examples due to the nature of the contrastive learning. VIbCReg can be used not only for time series but also for image data unlike the Franceschi. Note that VIbCReg reaches the same performance as VICReg on images while VIbCReg performs better than VICReg on time series. VIbCReg for visual representation learning is available at <https://github.com/vturrisi/solo-learn> which includes results on CIFAR-10, CIFAR-100, and ImageNet-100 along with other popular computer-vision SSL frameworks.

The performance ranking order remains the same in Table 2 and Table 5 for VIbCReg, SimCLR, VICReg, and Barlow Twins. But BYOL and SimSiam differ in their orders in the two tables. The main difference between the Part 1 and Part 2 experiments is the use of multi-crop with different crop sizes as introduced in Appendix A.3. Therefore, we deduce that SimSiam has a good synergistic effect with the multi-crop while BYOL has the opposite effect.

## 5 Limitation

VIbCReg is purposefully designed to stay similar to the computer-vision SSL frameworks so that it can be compatible with both images and time series. However, the current version of VIbCReg cannot process a very-long sequence due to a GPU memory limit since it employs the multi-crop where one crop with 50% length and another crop with 100% length of input time series. Also, the ResNet encoder is used for VIbCReg to comply with the computer-vision SSL frameworks. However, ResNet has a fixed receptive field size and can only process local information for long time series. Better performance is expected when an encoder that can enable various-sized receptive fields is used.

## 6 Conclusion

In this paper, we have evaluated the well-known Siamese-style computer vision SSL frameworks. The results show that even when the computer vision SSL frameworks are naively applied to a different modality (*i.e.*, time series), they can still result in effective representation learning. We argue that some of the design ideas from the computer vision SSL frameworks may be taken to develop a better representation learning method for time series in future work. We also introduce VIbCReg and it shows the robust performance while outperforming the others. The good performance of VIbCReg is achieved by inducing stronger

Table 5 Summary of the SVM accuracy on UCR.

Subset names	Sim CLR	BYOL	Sim Siam	Barlow Twins	VICReg	VibCReg	TimeNet [24]	Frances. [17]
ACSF1	0.833	0.770	0.883	0.817	0.840	0.897		0.885
Adiac	0.761	0.614	0.781	0.743	0.704	0.813	0.565	0.706
ArrowHead	0.815	0.792	0.792	0.737	0.731	0.811		0.805
Beef	0.489	0.678	0.711	0.511	0.667	0.733		0.667
BeetleFly	0.667	0.650	0.783	0.717	0.700	0.783		0.850
BirdChicken	0.950	0.900	0.933	0.900	0.933	0.933		0.813
BME	0.889	0.904	0.984	0.751	0.802	0.971		0.991
Car	0.778	0.717	0.789	0.594	0.711	0.861		0.746
CBF	0.990	0.937	0.990	0.924	0.886	0.992		0.987
Chinatown	0.958	0.921	0.972	0.956	0.914	0.954		0.949
ChlorineConcentration	0.604	0.563	0.748	0.589	0.628	0.762	0.723	0.739
CinCECGtorso	0.687	0.572	0.639	0.562	0.579	0.774		0.711
Coffee	0.988	0.988	0.964	0.881	0.917	0.976		0.991
Computers	0.711	0.653	0.777	0.669	0.689	0.785		0.668
CricketX	0.704	0.574	0.785	0.553	0.624	0.809	0.659	0.715
CricketY	0.729	0.544	0.767	0.562	0.621	0.811		0.692
CricketZ	0.752	0.602	0.811	0.550	0.626	0.828		0.716
Crop	0.720	0.700	0.740	0.676	0.759	0.744		0.726
DiatomSizeReduction	0.877	0.886	0.919	0.892	0.859	0.859		0.988
DistalPhalanxOutlineAgeGroup	0.741	0.736	0.717	0.727	0.727	0.743		0.728
DistalPhalanxOutlineCorrect	0.774	0.756	0.772	0.737	0.761	0.767		0.764
DistalPhalanxTW	0.662	0.655	0.650	0.671	0.662	0.652		0.678
Earthquakes	0.748	0.748	0.748	0.748	0.748	0.748		0.748
ECG200	0.863	0.867	0.853	0.820	0.873	0.850		0.893
ECG5000	0.940	0.934	0.931	0.930	0.937	0.935	0.934	0.937
ECGFiveDays	0.890	0.833	0.759	0.810	0.816	0.768		1.000
ElectricDevices	0.681	0.687	0.697	0.636	0.598	0.682	0.665	0.707
EOGHorizontalSignal	0.527	0.341	0.555	0.376	0.432	0.645		0.565
EOGVerticalSignal	0.366	0.283	0.373	0.320	0.311	0.405		0.419
EthanolLevel	0.416	0.432	0.301	0.439	0.550	0.308		0.364
FaceAll	0.740	0.699	0.760	0.676	0.712	0.800		0.773
FaceFour	0.856	0.720	0.909	0.894	0.814	0.924		0.847
FacesUCR	0.821	0.753	0.867	0.733	0.795	0.891		0.882
FiftyWords	0.673	0.500	0.709	0.560	0.565	0.759		0.739
Fish	0.865	0.832	0.937	0.775	0.785	0.981		0.899
FordA	0.949	0.655	0.956	0.877	0.923	0.952		0.925
FordB	0.854	0.826	0.848	0.728	0.814	0.846		0.787
FreezerRegularTrain	0.931	0.979	0.967	0.950	0.971	0.963		0.977
FreezerSmallTrain	0.744	0.910	0.762	0.762	0.725	0.877		0.941
Fungi								1.000
GunPoint	0.944	0.911	0.978	0.938	0.962	0.987		0.977
GunPointAgeSpan	0.960	0.961	0.966	0.977	0.957	0.980		0.989
GunPointMaleVersusFemale	0.997	0.996	0.997	0.996	0.988	0.999		0.999
GunPointOldVersusYoung	1.000	0.990	0.990	1.000	0.999	0.995		1.000
Ham	0.613	0.619	0.622	0.546	0.625	0.635		0.679
HandOutlines	0.894	0.796	0.886	0.753	0.876	0.907		0.918
Haptics	0.468	0.367	0.461	0.432	0.405	0.504		0.451
Herring	0.589	0.578	0.557	0.589	0.568	0.578		0.594
HouseTwenty	0.927	0.734	0.964	0.826	0.832	0.975		0.933
InlineSkate	0.353	0.310	0.406	0.358	0.286	0.446		0.413
InsectEPGRegularTrain	1.000	1.000	1.000	1.000	1.000	0.999		1.000
InsectEPGSmallTrain	1.000	0.941	1.000	1.000	0.989	0.996		1.000
InsectWingbeatSound	0.546	0.485	0.539	0.474	0.506	0.566		0.604
ItalyPowerDemand	0.951	0.926	0.936	0.898	0.928	0.942		0.937
LargeKitchenAppliances	0.848	0.752	0.875	0.761	0.739	0.876		0.814
Lightning2	0.732	0.738	0.732	0.650	0.656	0.749		0.857
Lightning7	0.653	0.571	0.667	0.598	0.708	0.689		0.809
Mallat	0.942	0.861	0.889	0.866	0.903	0.871		0.948
Meat	0.894	0.950	0.906	0.911	0.928	0.861		0.900
MedicalImages	0.749	0.700	0.760	0.674	0.726	0.764	0.753	0.757
MelbournePedestrian	0.921	0.903	0.906	0.861	0.930	0.918		0.946
MiddlePhalanxOutlineAgeGroup	0.565	0.630	0.606	0.545	0.580	0.571		0.648
MiddlePhalanxOutlineCorrect	0.694	0.758	0.806	0.788	0.821	0.780		0.792
MiddlePhalanxTW	0.604	0.530	0.593	0.582	0.584	0.593		0.604
MixedShapesRegularTrain	0.945	0.865	0.961	0.928	0.876	0.962		0.908
MixedShapesSmallTrain	0.872	0.727	0.885	0.805	0.748	0.905		0.863
MoteStrain	0.815	0.789	0.877	0.747	0.820	0.871		0.862
NonInvasiveFetalECGThorax1	0.809	0.758	0.777	0.834	0.886	0.832		0.901
NonInvasiveFetalECGThorax2	0.881	0.837	0.857	0.879	0.903	0.910		0.922
OliveOil	0.733	0.844	0.744	0.811	0.800	0.811		0.859
OSULeaf	0.851	0.642	0.868	0.726	0.679	0.895		0.742
PhalangesOutlinesCorrect	0.746	0.625	0.797	0.646	0.737	0.818	0.772	0.796
Phoneme	0.292	0.201	0.315	0.215	0.239	0.325		0.464
PigAirwayPressure								0.921
PigArtPressure								0.921
PigCVP								0.590
Plane	0.987	0.971	0.978	0.975	0.978	0.990		0.992
PowerCons	0.970	0.931	0.957	0.957	0.974	0.980		0.925
ProximalPhalanxOutlineAgeGroup	0.839	0.834	0.850	0.826	0.837	0.844		0.849
ProximalPhalanxOutlineCorrect	0.795	0.794	0.834	0.795	0.847	0.866		0.862
ProximalPhalanxTW	0.772	0.771	0.802	0.797	0.795	0.789		0.793
RefrigerationDevices	0.500	0.500	0.516	0.498	0.528	0.531		0.525
Rock	0.440	0.447	0.447	0.453	0.400	0.687		0.600
ScreenType	0.517	0.421	0.524	0.434	0.460	0.561		0.416
SemgHandGenderCh2	0.877	0.730	0.877	0.849	0.880	0.847		0.865

**Table 6** Summary of the SVM accuracy on UCR (continued).

Subset names	Sim CLR	BYOL	Sim Siam	Barlow Twins	VICReg	VibCReg	TimeNet [24]	Frances. [17]
SemgHandMovementCh2	0.779	0.596	0.739	0.650	0.684	0.676		0.712
SemgHandSubjectCh2	0.842	0.666	0.821	0.768	0.808	0.805		0.822
ShapeletSim	0.720	0.622	0.767	0.857	0.574	0.757		0.674
ShapesAll	0.856	0.696	0.882	0.751	0.776	0.910		0.848
SmallKitchenAppliances	0.795	0.696	0.837	0.721	0.728	0.834		0.685
SmoothSubspace	0.813	0.847	0.776	0.820	0.853	0.862		0.948
SonyAIBORobotSurface1	0.784	0.722	0.733	0.772	0.708	0.818		0.893
SonyAIBORobotSurface2	0.884	0.730	0.923	0.757	0.832	0.860		0.909
StarLightCurves	0.972	0.936	0.978	0.961	0.960	0.977		0.962
Strawberry	0.957	0.939	0.954	0.932	0.959	0.963		0.951
SweedishLeaf	0.934	0.835	0.947	0.902	0.893	0.961	0.901	0.918
Symbols	0.928	0.731	0.960	0.891	0.896	0.975		0.949
SyntheticControl	0.983	0.958	0.978	0.939	0.959	0.979	0.983	0.984
ToeSegmentation1	0.942	0.789	0.953	0.655	0.731	0.936		0.925
ToeSegmentation2	0.815	0.738	0.900	0.662	0.731	0.903		0.875
Trace	0.987	0.920	1.000	0.993	0.963	0.997		0.998
TwoLeadECG	0.762	0.706	0.934	0.797	0.713	0.911	0.999	0.996
TwoPatterns	0.990	0.997	0.975	0.675	0.906	0.993		0.999
UMD	0.877	0.833	0.977	0.875	0.852	0.979		0.988
UWaveGestureLibraryAll	0.924	0.730	0.883	0.780	0.790	0.918		0.895
UWaveGestureLibraryX	0.802	0.715	0.795	0.677	0.741	0.801		0.794
UWaveGestureLibraryY	0.747	0.631	0.749	0.598	0.649	0.757		0.711
UWaveGestureLibraryZ	0.755	0.662	0.755	0.621	0.706	0.764		0.743
Wafer	0.991	0.988	0.991	0.983	0.992	0.991	0.994	0.993
Wine	0.772	0.722	0.765	0.617	0.772	0.846		0.797
WordSynonyms	0.496	0.428	0.532	0.427	0.511	0.678		0.661
Worms	0.758	0.606	0.792	0.610	0.684	0.788		0.704
WormsTwoClass	0.827	0.706	0.831	0.688	0.719	0.827		0.763
Yoga	0.849	0.776	0.884	0.759	0.817	0.896	0.866	0.837
Mean Rank	3.6	5.7	3.2	5.5	4.7	2.5		2.8

**Table 7** Summary of the SVM accuracy on UEA.

Subset names	Sim CLR	BYOL	Sim Siam	Barlow Twins	VICReg	VibCReg	Frances. [17]
ArticulatoryWordRecognition	0.934	0.883	0.861	0.744	0.889	0.956	0.961
AtrialFibrillation	0.311	0.400	0.289	0.267	0.378	0.311	0.133
BasicMotions	0.983	0.850	0.983	0.992	0.900	1.000	1.000
Cricket	0.963	0.884	0.968	0.931	0.944	0.968	0.967
DuckDuckGeese	0.393	0.313	0.473	0.307	0.360	0.513	0.642
EigenWorms							0.837
Epilepsy	0.961	0.829	0.964	0.915	0.942	0.973	0.971
ERing	0.862	0.848	0.844	0.798	0.859	0.901	0.133
EthanolConcentration	0.294	0.307	0.319	0.270	0.279	0.304	0.248
FaceDetection							0.520
FingerMovements	0.513	0.497	0.527	0.540	0.530	0.520	0.540
HandMovementDirection	0.311	0.315	0.356	0.275	0.297	0.360	0.320
Handwriting	0.325	0.319	0.433	0.188	0.262	0.472	0.454
Heartbeat	0.711	0.722	0.720	0.719	0.717	0.750	0.743
Libras	0.850	0.667	0.857	0.735	0.748	0.863	0.881
LSST	0.515	0.412	0.557	0.389	0.482	0.577	0.532
MotorImagery	0.450	0.513	0.540	0.573	0.520	0.493	0.550
NATOPS	0.802	0.678	0.759	0.750	0.724	0.839	0.922
PEMS-SF	0.809	0.798	0.726	0.842	0.829	0.682	0.661
PenDigits							0.982
Phoneme	0.302	0.203	0.332	0.250	0.229	0.315	0.217
RacketSports	0.789	0.739	0.803	0.671	0.728	0.789	0.822
SelfRegulationSCP1	0.716	0.755	0.732	0.784	0.779	0.724	0.821
SelfRegulationSCP2	0.552	0.496	0.506	0.539	0.546	0.513	0.543
StandWalkJump							0.355
UWaveGestureLibrary	0.817	0.685	0.801	0.591	0.625	0.861	0.876
Mean Rank	4.1	5.2	3.5	5.1	4.5	2.7	2.9

feature decorrelation with a normalized covariance and iterative normalization layer.

**Acknowledgments.** We would like to thank the Norwegian Research Council for funding the Machine Learning for Irregular Time Series (ML4ITS) project (312062). This funding directly supported this research.

## 7 Statements and Declarations

### *Funding*

This research is funded by the Norwegian Research Council for funding the Machine Learning for Irregular Time Series (ML4ITS) project (312062).

### *Conflicts of interest/Competing interests*

Not applicable.

### *Ethics approval*

Not applicable.

### *Consent to participate*

Not applicable.

### *Consent for publication*

Not applicable.

### *Availability of data and materials*

The used datasets are popular open-source bench mark datasets and the used deep learning library is an open-source Python deep learning library named PyTorch.

### *Authors' Contributions*

1. Daesoo Lee: Proposed a first draft of the proposed method and improved the proposal and implemented the proposal with his supervisor, Prof. Erlend Aune. And Daesoo worked on the paper with Prof. Aune.
2. Erlend Aune: Improved the initial proposal and implemented the proposal and wrote the paper with Daesoo.

## Appendix A Implementation Details

**Table A1** PyTorch-style pseudocode for VlbCReg. We mostly follow the same notations from the VICReg paper.

---

**Algorithm 1** PyTorch-style pseudocode for VlbCReg

---

```

# f: encoder network
# lambda_, mu, nu: coefficients of the invariance, variance,
#               and covariance losses
# N: batch size
# F: feature size (= dimension of the representations)
#
# mse_loss: Mean square error loss function
# off_diagonal: off-diagonal elements of a matrix
# relu: ReLU activation function
# normalize: torch.nn.functional.normalize(..)

for x in loader: # load a batch with N samples
    # two randomly augmented versions of x
    x_a, x_b = augment(x)

    # compute representations
    z_a = f(x_a) # N x F
    z_b = f(x_b) # N x F

    # invariance loss
    sim_loss = mse_loss(z_a, z_b)

    # variance loss
    std_z_a = torch.sqrt(z_a.var(dim=0) + 1e-4)
    std_z_b = torch.sqrt(z_b.var(dim=0) + 1e-4)
    std_loss = torch.mean(relu(1 - std_z_a))
    std_loss = std_loss + torch.mean(relu(1 - std_z_b))

    # covariance loss
    z_a = z_a - z_a.mean(dim=0)
    z_b = z_b - z_b.mean(dim=0)
    norm_z_a = normalize(z_a, p=2, dim=0)
    norm_z_b = normalize(z_b, p=2, dim=0)
    norm_cov_z_a = (norm_z_a.T @ norm_z_a)
    norm_cov_z_b = (norm_z_b.T @ norm_z_b)
    norm_cov_loss = (off_diagonal(norm_cov_z_a)**2).mean() \
                    + (off_diagonal(norm_cov_z_b)**2).mean()

    # loss
    loss = lambda_ * sim_loss + mu * std_loss + nu * norm_cov_loss

    # optimization step
    loss.backward()
    optimizer.step()

```

---

## A.1 Encoder

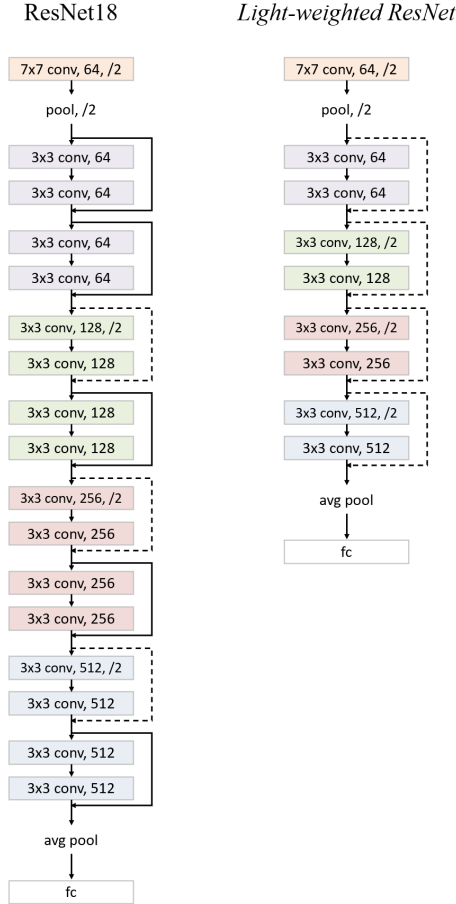


**Fig. A1** The light-weighted ResNet is illustrated compared to ResNet18.

## A.2 SSL Frameworks

In our experiments, the SSL frameworks are implemented as close as possible to the original implementations. The only major difference is the encoder’s dimension. Instead of 2-dimensional image input, they receive 1-dimensional time series input. Unless specified differently, the architectures follow original implementations.

### *SimCLR*

Projector’s dimension size is set to 4096.  $\tau$  is set to 0.1.

***BYOL***

Projector’s dimension size is set to 512. The momentum of 0.9 is used.

***SimSiam***

All the settings are the same as its original implementation.

***Barlow Twins***

Projector’s dimension size is set to 4096.  $\lambda$  is set to  $5 \cdot 10^{-3}$ .

***VICReg***

Projector’s dimension size is set to 4096.  $\lambda$ ,  $\mu$ , and  $\nu$  are set to 25, 25, and 1, respectively.

***VibCReg***

Its projector consists as follows: (Linear-BN-ReLU)-(Linear-BN-ReLU)-(Linear-IterNorm), where Linear, BN, and ReLU denotes a linear layer, batch normalization [35], and rectified linear unit, respectively. The dimension of the inner and output layers of the projector is set to 4096.  $\lambda$  and  $\mu$  are set to 25 and 25, respectively.  $\nu$  is set to 200 for the part-1 evaluation and 100 for the part-2 evaluation.

***TNC***

Its discriminator consists as follows: Linear-ReLU-Dropout(0.5)-Linear, following its original implementation in GitHub ([https://github.com/sanatonek/TNC\\_representation\\_learning](https://github.com/sanatonek/TNC_representation_learning)). The discriminator’s input dimension size is 2 times the representation size and its hidden layer’s dimension size is 4 times the representation size.  $w$  is set to 0.05. As for selecting its positive and negative examples, a time step for a reference example is first randomly sampled. Note that the reference example is a random crop with the sampled time step at the center. Then, a time step for a positive example is sampled according to a normal distribution with mean of the time step of the reference example and standard deviation of crop length/4. A time step for a negative example is sampled outside of the normal distribution for the positive example.

**A.3 Data Augmentation Methods*****Data Augmentation for Experimental Evaluation Part 1***

In the part-1 evaluation, three data augmentation methods are used for training: **Random Crop**, **Random Amplitude Resize**, and **Random Vertical Shift**, and **Random Amplitude Resize** and **Random Vertical Shift** are used for the linear evaluation.

**Random Crop** is similar to the one in computer vision. The only difference is that the random crop is conducted on 1D time series data in our experiments. Its hyperparameter is crop size. The crop size for the UCR datasets



in the part-1 evaluation is presented in Table A2. Different datasets have different patterns to be distinguishable with respect to different classes. Some have long patterns while some have short patterns. Depending on length of distinguishable patterns, ideal crop size may differ. For the crop length in the table, the ones that result in better performance are chosen. A more generic approach is used in the part-2 evaluation.

**Table A2** Summary of the crop size for each UCR dataset.

Dataset name	Length	Use half length for crop	Crop size
Crop	46	x	46
ElectricDevices	96	o	48
StarLightCurves	1024	o	512
Wafer	152	x	152
ECG5000	140	o	70
TwoPatterns	128	o	64
FordA	500	o	250
UWaveGestureLibraryAll	945	o	473
FordB	500	o	250
ChlorineConcentration	166	x	166
ShapesAll	512	o	256
FiftyWords	270	o	135
NonInvasiveFetalECGThorax1	750	x	750
Phoneme	1024	o	512
WordSynonyms	270	o	135

**Random Amplitude Resize** randomly resizes overall amplitude of input time series. It is expressed as Eq. (A1), where  $m_{\text{rar}}$  is a multiplier to input time series  $x$ , and  $\alpha_{\text{rar}}$  is a hyperparameter.  $\alpha_{\text{rar}}$  is set to 0.3.

$$x = m_{\text{rar}} x; \quad m_{\text{rar}} \sim \text{U}(1 - \alpha_{\text{rar}}, 1 + \alpha_{\text{rar}}) \quad (\text{A1})$$

**Random Vertical Shift** randomly shifts input time series in a vertical direction. It is expressed as Eq. (A2), where  $x'$  denotes input time series before any augmentation, Std denotes a standard deviation estimator, and  $\beta_{\text{rvs}}$  is a hyperparameter to determine a magnitude of the vertical shift.  $\beta_{\text{rvs}}$  is set to 0.5.

$$x = x + s_{\text{rvs}}; \quad s_{\text{rvs}} \sim \text{U}(-\alpha_{\text{rvs}}, \alpha_{\text{rvs}}) \quad (\text{A2})$$

$$\alpha_{\text{rvs}} = \beta_{\text{rvs}} \text{Std}(x') \quad (\text{A3})$$

### Data Augmentation for Experimental Evaluation Part 2

In the part-2 evaluation, two data augmentation methods are used: **Random Crop** and **Random Amplitude Resize**.

**Random Crop**

Instead of using the better crop length between 50% and 100% of time series length, both are used in the part-2 evaluation such that the invariance, variance, and the covariance loss are computed twice for two different input pairs with different crop lengths to allow different views for the models. It is inspired by [36] that proposed SwAV, and they experimentally show that using multiple crops with different sizes helps to produce better representations. Then, the loss function is computed as in Table A3.

**Table A3** Pseudocode for ViBcReg with Random Crop with two different crop lengths. The notation follows the pseudocode for ViBcReg in Table A1. Note that `crop_length_ratio` represents different crop lengths: 0.5 and 1.0 denote 50% and 100%, respectively.

---

**Algorithm 2** PyTorch-style pseudocode for ViBcReg with **Random Crop** with two different crop lengths

---

```

for x in loader: # load a batch with N samples
    for crop_length_ratio in [0.5, 1.0]:
        # two randomly augmented versions of x
        # with crop length of 50% or 100% of time series.
        x_a, x_b = augment(x, crop_length_ratio)

        # compute representations
        z_a = f(x_a) # N x F
        z_b = f(x_b) # N x F

        # loss
        invar_loss = variance_loss(z_a, z_b)
        var_loss = variance_loss(z_a, z_b)
        cov_loss = covariance_loss(z_a, z_b)
        loss = lambda_ * invar_loss + mu * var_loss + nu * cov_loss

        # optimization step
        loss.backward()
        optimizer.step()

```

---

**Random Amplitude Resize** is slightly different in the part-2 evaluation from the part-1 evaluation as Eq. (A4).  $\alpha_{\text{rar}}$  is set to 0.1.

$$x = m_{\text{rar}} x; \quad m_{\text{rar}} \sim N(0, \alpha_{\text{rar}}) \quad (\text{A4})$$

## Appendix B FD and FcE Metrics

FD and FcE metrics are metrics for the feature decorrelation and feature component expressiveness. They are used to keep track of FD and FcE status of learned features during SSL for representation learning. The FD metric and FcE metric are defined in Eq. (B6) and Eq. (B7), respectively.  $Z$  is output from the projector and  $F$  is feature size of  $Z$ .  $\sum_{i \neq j}$  denotes ignoring the diagonal terms in the matrix. In Eq. (B5), the l2-norm is conducted along the batch dimension. In Eq. (B7), Std denotes a standard deviation estimator and it is conducted along the batch dimension.

$$C(Z) = \left( \frac{Z - \bar{Z}}{\|Z - \bar{Z}\|_2} \right)^T \left( \frac{Z - \bar{Z}}{\|Z - \bar{Z}\|_2} \right) \quad (\text{B5})$$

$$\mathcal{M}_{\text{FD}} = \frac{1}{F^2} \sum_{i \neq j} |C(Z)| \quad (\text{B6})$$

$$\mathcal{M}_{\text{FcE}} = \frac{1}{F} \sum_{f=1}^F \text{Std}(Z) \quad (\text{B7})$$

## Appendix C Additional Result Materials

### *Faster Representation Learning by VlbCReg*

The FD and FcE metrics that correspond to Fig. 4 (*i.e.*, 5-kNN classification accuracy on the UCR datasets) are presented in Figs. C2-C3, respectively.

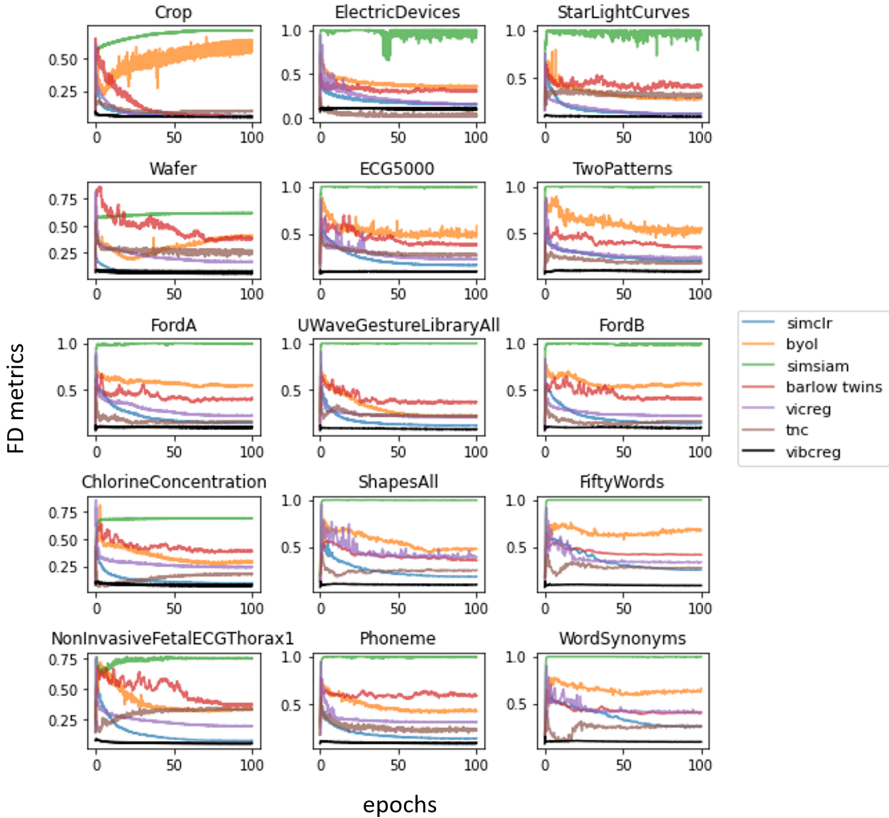


**Fig. C2** FD metric on the UCR datasets during the representation learning. It is noticeable that the metric of VlbCReg converges to near-zero in the beginning, ensuring the feature decorrelation throughout the entire training epochs.

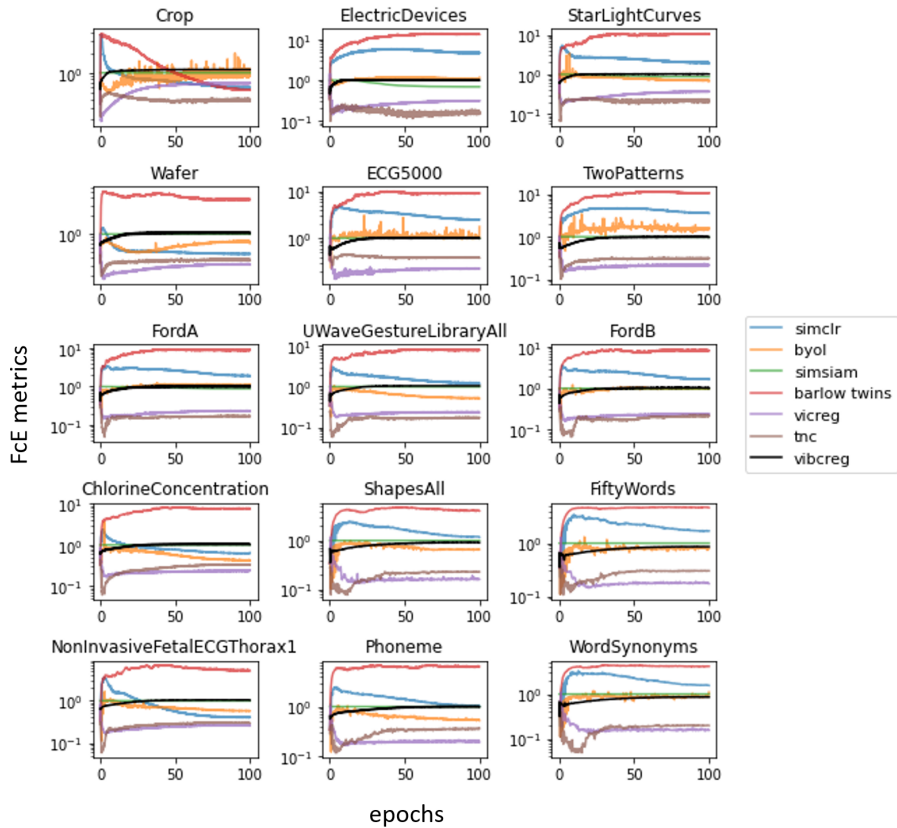


**Fig. C3** FcE metric on the UCR datasets during the representation learning. Note that y-axis is log-scaled. It can be observed that the metric of VlbCReg converges to 1 fairly quickly, ensuring the feature component expressiveness throughout the entire training epochs.

## References

- [1] Hénaff, O.J., Razavi, A., Doersch, C., Ali Eslami, S.M., Van Den Oord, A.: Data-efficient image recognition with contrastive predictive coding. In: International Conference on Machine Learning (2019)
- [2] Chen, T., Kornblith, S., Norouzi, M., Hinton, G.: A simple framework for contrastive learning of visual representations. In: International Conference on Machine Learning, pp. 1597–1607 (2020). PMLR
- [3] He, K., Fan, H., Wu, Y., Xie, S., Girshick, R.: Momentum contrast for unsupervised visual representation learning. In: Proceedings of the IEEE/CVF Conference on Computer Vision and Pattern Recognition, pp. 9729–9738 (2020)
- [4] Grill, J.-B., Strub, F., Alché, F., Tallec, C., Richemond, P.H.,

Buchatskaya, E., Doersch, C., Pires, B.A., Guo, Z.D., Azar, M.G., et al.: Bootstrap your own latent: A new approach to self-supervised learning. arXiv preprint arXiv:2006.07733 (2020)

- [5] Chen, X., He, K.: Exploring simple siamese representation learning (2020)
- [6] Zbontar, J., Jing, L., Misra, I., Lecun, Y., Deny, S.: Barlow Twins: Self-Supervised Learning via Redundancy Reduction. In: arXiv (2021). <https://github.com/facebookresearch/barlowtwins>
- [7] Bardes, A., Ponce, J., LeCun, Y.: VICReg: Variance-Invariance-Covariance Regularization for Self-Supervised Learning. In: arXiv (2021). <http://arxiv.org/abs/2105.04906>
- [8] Koch, G., Zemel, R., Salakhutdinov, R.: Siamese Neural Networks for One-Shot Image Recognition. In: ICML - Deep Learning Workshop, vol. 7, pp. 956–963 (2015)
- [9] Makridakis, S., Spiliotis, E., Assimakopoulos, V.: The m4 competition: Results, findings, conclusion and way forward. *International Journal of Forecasting* **34**(4), 802–808 (2018)
- [10] Makridakis, S., Spiliotis, E., Assimakopoulos, V.: The m5 accuracy competition: Results, findings and conclusions. *International Journal of Forecasting* (2020)
- [11] Chen, Y., Keogh, E., Hu, B., Begum, N., Bagnall, A., Mueen, A., Batista, G.: The UCR Time Series Classification Archive (2015)
- [12] Bagnall, A., Dau, H.A., Lines, J., Flynn, M., Large, J., Bostrom, A., Southam, P., Keogh, E.: The uea multivariate time series classification archive, 2018. arXiv preprint arXiv:1811.00075 (2018)
- [13] Ermolov, A., Siarohin, A., Sangineto, E., Sebe, N.: Whitening for Self-Supervised Representation Learning (2020). <https://github.com/htdt/>
- [14] Hua, T., Wang, W., Xue, Z., Wang, Y., Ren, S., Zhao, H.: On Feature Decorrelation in Self-Supervised Learning. In: arXiv (2021). <http://arxiv.org/abs/2105.00470>
- [15] Chen, T., Kornblith, S., Norouzi, M., Hinton, G.: A simple framework for contrastive learning of visual representations (2020)
- [16] Huang, L., Yang, D., Lang, B., Deng, J.: Decorrelated Batch Normalization. In: Proceedings of the IEEE Computer Society Conference on Computer Vision and Pattern Recognition, pp. 791–800 (2018). <https://doi.org/10.1109/CVPR.2018.00089>

- [17] Franceschi, J.-Y., Dieuleveut, A., Jaggi, M.: Unsupervised scalable representation learning for multivariate time series. *Advances in neural information processing systems* **32** (2019)
- [18] Chopra, S., Hadsell, R., LeCun, Y.: Learning a similarity metric discriminatively, with application to face verification. In: *Proceedings - 2005 IEEE Computer Society Conference on Computer Vision and Pattern Recognition, CVPR 2005*, vol. I, pp. 539–546 (2005). <https://doi.org/10.1109/CVPR.2005.202>. <https://ieeexplore.ieee.org/abstract/document/1467314/>
- [19] Van Den Oord, A., Li, Y., Vinyals, O.: Representation learning with contrastive predictive coding (2018)
- [20] He, K., Zhang, X., Ren, S., Sun, J.: Deep residual learning for image recognition. In: *Proceedings of the IEEE Computer Society Conference on Computer Vision and Pattern Recognition*, vol. 2016-Decem, pp. 770–778 (2016). <https://doi.org/10.1109/CVPR.2016.90>. <http://image-net.org/challenges/LSVRC/2015/>
- [21] Wu, Z., Xiong, Y., Yu, S.X., Lin, D.: Unsupervised Feature Learning via Non-parametric Instance Discrimination. In: *Proceedings of the IEEE Computer Society Conference on Computer Vision and Pattern Recognition*, pp. 3733–3742 (2018). <https://doi.org/10.1109/CVPR.2018.00393>
- [22] Dereniowski, D., Kubale, M.: Cholesky factorization of matrices in parallel and ranking of graphs. In: *International Conference on Parallel Processing and Applied Mathematics*, vol. 3019, pp. 985–992 (2003). <https://doi.org/10.1007/978-3-540-24669-5{-}>
- [23] Siarohin, A., Sangineto, E., Sebe, N.: Whitening and coloring batch transform for GANS. In: *7th International Conference on Learning Representations, ICLR 2019* (2019). <https://github.com/AliaksandrSiarohin/wc-gan>.
- [24] Malhotra, P., TV, V., Vig, L., Agarwal, P., Shroff, G.: Timenet: Pre-trained deep recurrent neural network for time series classification. *arXiv preprint arXiv:1706.08838* (2017)
- [25] Dempster, A., Petitjean, F., Webb, G.I.: Rocket: exceptionally fast and accurate time series classification using random convolutional kernels. *Data Mining and Knowledge Discovery* **34**(5), 1454–1495 (2020)
- [26] Sutskever, I., Vinyals, O., Le, Q.V.: Sequence to sequence learning with neural networks. *Advances in neural information processing systems* **27** (2014)
- [27] Lea, C., Vidal, R., Reiter, A., Hager, G.D.: Temporal convolutional

- networks: A unified approach to action segmentation. In: European Conference on Computer Vision, pp. 47–54 (2016). Springer
- [28] Huang, L., Zhou, Y., Zhu, F., Liu, L., Shao, L.: Iterative normalization: Beyond standardization towards efficient whitening. In: Proceedings of the IEEE Computer Society Conference on Computer Vision and Pattern Recognition, vol. 2019-June, pp. 4869–4878 (2019). <https://doi.org/10.1109/CVPR.2019.00501>
- [29] Wang, F.: Multi-Scale-1D-ResNet. GitHub (2018)
- [30] Loshchilov, I., Hutter, F.: Decoupled weight decay regularization. In: 7th International Conference on Learning Representations, ICLR 2019 (2019). <https://github.com/loshchil/AdamW-and-SGDW>
- [31] Loshchilov, I., Hutter, F.: SGDR: Stochastic gradient descent with warm restarts. In: 5th International Conference on Learning Representations, ICLR 2017 - Conference Track Proceedings (2017). <https://github.com/loshchil/SGDR>
- [32] Paszke, A., Gross, S., Massa, F., Lerer, A., Bradbury, J., Chanan, G., Killeen, T., Lin, Z., Gimelshein, N., Antiga, L., Desmaison, A., Kopf, A., Yang, E., DeVito, Z., Raison, M., Tejani, A., Chilamkurthy, S., Steiner, B., Fang, L., Bai, J., Chintala, S.: Pytorch: An imperative style, high-performance deep learning library. In: Wallach, H., Larochelle, H., Beygelzimer, A., d'Alché-Buc, F., Fox, E., Garnett, R. (eds.) Advances in Neural Information Processing Systems 32, pp. 8024–8035 (2019). <http://papers.neurips.cc/paper/9015-pytorch-an-imperative-style-high-performance-deep-learning-library.pdf>
- [33] Koohpayegani, S.A., Tejankar, A., Pirsiavash, H.: Mean Shift for Self-Supervised Learning. In: arXiv (2021). <https://github.com/UMBCvision/MSF> <http://arxiv.org/abs/2105.07269>
- [34] Xie, Z., Zhang, Z., Cao, Y., Lin, Y., Bao, J., Yao, Z., Dai, Q., Hu, H.: Simsim: A simple framework for masked image modeling. In: Proceedings of the IEEE/CVF Conference on Computer Vision and Pattern Recognition, pp. 9653–9663 (2022)
- [35] Ioffe, S., Szegedy, C.: Batch normalization: Accelerating deep network training by reducing internal covariate shift. In: 32nd International Conference on Machine Learning, ICML 2015, vol. 1, pp. 448–456 (2015)
- [36] Caron, M., Misra, I., Mairal, J., Goyal, P., Bojanowski, P., Joulin, A.: Unsupervised learning of visual features by contrasting cluster assignments. Advances in Neural Information Processing Systems **33**, 9912–9924 (2020)